Contribution from the Anorganisch Chemisch Laboratorium and the Laboratorium voor Kristallografie, University of Amsterdam, J. H. van't Hoff Instituut, 1018 WV Amsterdam, The Netherlands

Influence of α Branching of the 1,4-Substituents on the Coordination of 1,4-Diazabutadienes in Mono-, Bi-, Tri-, and Tetranuclear Ruthenium Carbonyl Complexes. Crystal Structure of [σ-N,σ-N′,η^2-C=N,η^2-C=N′-Diglyoxal bis(isopropylimine)]octacarbonyltetraruthenium

L. H. STAAL, L. H. POLM, K. VRIEZE,* F. PLOEGER, and C. H. STAM

Received November 25, 1980

A series of 1,4-diazabutadienes (DAB) has been reacted with $Ru_3(CO)_{12}$, resulting in the formation of $Ru(CO)_3(DAB)$, $Ru_2(CO)_6(DAB)$, $Ru_3(CO)_8(DAB)$, and $Ru_4(CO)_8(DAB)_2$. The actual complex formed depends upon the reaction conditions and the α branching of the substituents attached to the DAB ligand. The crystal structure of $Ru_4(CO)_8$[glyoxal bis(isopropylimine)]$_2$ has been determined. The crystals are monoclinic with space group *Pn*. The cell constants are a = 9.506 (1) Å, b = 9.952 (3) Å, c = 16.625 (4) Å, β = 94.975°, and Z = 2. A total of 3241 reflections have been used for the refinement, resulting in R = 4.8% for 360 parameters varied. The metal atoms in the cluster were found in a butterfly arrangement with five intermetallic bond distances ranging from 2.838 (2) to 2.994 (2) Å. The two DAB ligands act as 8e donors, donating two pairs of π electrons of the N=C=N skeleton and two lone pairs. The four pairs of π electrons of the two DAB ligands are donated to the same ruthenium atom which does not contain carbonyl groups. The cluster contains a $Ru(CO)_4$ fragment which is not bonded to the DAB ligands. On the bases of electron counting and ^{1}H NMR results, it was concluded that the DAB ligands in the $Ru_3(CO)_8(DAB)$ complexes are also in the 8e-donor mode. Low-temperature ^{1}H NMR data of the $Ru_4(CO)_8(DAB)_2$ clusters indicated the occurrence of an intramolecular exchange process of the butterfly core. For $Ru_4(CO)_8$[glyoxal bis(cyclohexylimine)]$_2$, one set of resonances is found at room temperature for the two ligand halves. At low temperature two distinct sets are observed, indicating two inequivalent ligand halves. The activation energy for the exchange process depends upon the substituents attached to the imine nitrogen atoms and decreases with increasing bulkiness.

Introduction

The versatile coordination behavior of 1,4-diazabutadienes (1,4-diazabutadienes are α-diimines; the abbreviation used throughout this paper is DAB) is a well-established feature.[12]

DAB ligands possess in principle eight electrons which can participate in coordination: two lone pairs on the nitrogen atoms and two pairs of π electrons. Recently the first example of the 8e-donor mode of the DAB ligand, i.e., σ-N,σ-N′,η^2-C=N,η^2-C=N′ coordination, has been established by a single-crystal structure determination.[2,3] Coordination of only one of the pairs of π electrons in addition to the two lone pairs has been observed in a series of binuclear metal carbonyl complexes in which the DAB acts as a six-electron donor: $M_2(CO)_6(DAB)$ (M = M′ = Fe,[4] Ru,[5] Os;[6] M = Fe and M′ = Ru;[7] M = Mn, Re and M′ = Co[8]).

The large number of complexes in which 1,4-diazabutadienes acts as σ,σ-bidentate ligands reflects that σ-N,σ-N′ coordination of the DAB ligand is a favorable situation.

Very little is known about the factors by which the coordination mode of the DAB ligands can be influenced. It has been shown that the geometry of the coordination polyhedron is an important factor[9] and that the stability of the metal–carbonyl bonds is also of crucial importance.[8]

In this paper we describe the influence of the substituents attached to the imine nitrogen atoms on the coordination mode of the DAB ligands in mono-, bi-, tri-, and tetranuclear ruthenium carbonyl DAB complexes.

Experimental Section

^{1}H NMR spectra were recorded with a Varian T60 and a Varian XL-100 apparatus, IR spectra have been recorded with a Perkin-Elmer 283 spectrophotometer, and mass spectra have been recorded with a Varian MAT 711 mass spectrometer, applying the field-desorption technique.

Elemental analyses were carried out by the section elemental analysis of the Institute for Organic Chemistry, TNO, Utrecht, The Netherlands.

$Ru_3(CO)_{12}$ was purchased from Strem Chemical and was used without purification. Glyoxal bis(isopropylimine), glyoxal bis(*tert*-butylimine), glyoxal bis(cyclohexylimine), and glyoxal bis(mesitylimine) were prepared according to standard procedures.[10–12]

All solvents were carefully dried and distilled prior to use. Reactions were carried out in an atmosphere of pure nitrogen. Silica used for column chromatography was dried, deoxygenated, and activated by heating to 180 °C under vacuum for 3 h.

Preparation of Glyoxal Bis(diisopropylmethylimine) (2,9-Dimethyl-3,8-diisopropyl-4,7-diazadeca-4,6-diene). An aqueous solution of glyoxal (17.5 mL, 100 mmol) was added dropwise to a stirred solution of 3-amino-2,4-dimethylpentane in ether (200 mmol in 300 mL of diethyl ether). The reaction mixture was stirred for 3 h, and the ether solution was washed three times with 100 mL of water. The solution was dried by stirring with anhydrous $MgSO_4$, and after filtration the solution was concentrated to 100 mL. The crude product was obtained by crystallization at −70 °C. Recrystallization from pentane yielded 80% of colorless crystals.

Preparation of Glyoxal Bis(isobutylimine) (2,9-Dimethyl-4,7-diazadeca-4,6-diene). An aqueous solution of glyoxal (8.75 mL, 50 mmol) was added dropwise to a stirred solution of isobutylamine (100 mmol in 150 mL of diethyl ether) at 0 °C. The reaction mixture was stirred for 3 h at room temperature, and the ether solution was washed twice with 50 mL of water. The solution was dried by stirring with anhydrous $MgSO_4$, and after filtration the ether was removed from the crude product by suction. A yellow oil was obtained from which the product was distilled under vacuum (90 °C, 1 mm), giving a colorless liquid; yield 60%.

*To whom correspondence should be addressed at the Anorganisch Chemisch Laboratorium.

(1) Staal, L. H.; Oskam, A.; Vrieze, K.; Roosendaal, E.; Schenk, H. *Inorg. Chem.* **1979**, *18*, 1634–1640.
(2) Staal, L. H.; van Koten, G.; Vrieze, K.; Ploeger, F.; Stam, C. H. *Inorg. Chem.* **1981**, *20*, 1830–1835.
(3) Staal, L. H.; Polm, L. H.; Vrieze, K.; Ploeger, F.; Stam, C. H. *J. Organomet. Chem.* **1980**, *199*, C13–C16.
(4) Frühauf, H. W.; Landers, A.; Goddard, R.; Krüger, C. *Angew. Chem.* **1978**, *90*, 56–58.
(5) Staal, L. H.; Polm, L. H.; Balk, R. W.; van Koten, G.; Vrieze, K.; Brouwers, A. M. F. *Inorg. Chem.* **1980**, *19*, 3343–3351.
(6) Staal, L. H.; van Koten, G.; Vrieze, K. *J. Organomet. Chem.* **1981**, *206*, 99–108.
(7) Staal, L. H.; Polm, L. H.; van Koten, G.; Vrieze, K. *Inorg. Chim. Acta* **1979**, *37*, L485–L487.
(8) Staal, L. H.; Keijsper, J.; van Koten, G.; Vrieze, K.; Cras, J. A.; Bosman, W. *Inorg. Chem.* **1981**, *20*, 555–562.
(9) Staal, L. H.; Bosma, P.; Vrieze, K. *Inorg. Chim. Acta* **1980**, *43*, 125–134.
(10) Bock, H.; tom Dieck, H. *Chem. Ber.* **1967**, *100*, 228–246.
(11) Kliegman, J. M.; Barnes, R. K. *J. Org. Chem.* **1970**, *35*, 3140–3143.
(12) Kliegman, J. M.; Barnes, R. K. *Tetrahedron* **1970**, *26*, 2555–2560.

0020-1669/81/1320-3590$01.25/0

Table I. Atomic Coordinates of $Ru_4(CO)_8$[glyoxal bis(isopropylimine)]$_2$ (Esd's in Parentheses)

	x	y	z		x	y	z
Ru(1)	0.14067 (14)	0.09593 (13)	0.12211 (8)	C(17)	0.5549 (27)	−0.1751 (22)	0.1928 (12)
Ru(2)	0.39134 (12)	0.17469 (13)	0.21657 (8)	C(18)	0.2801 (26)	−0.2692 (18)	0.1413 (16)
Ru(3)	0.10877 (12)	0.17503 (13)	0.28327 (8)	C(19)	−0.0486 (22)	0.3832 (17)	0.1569 (16)
Ru(4)	0.35892 (14)	0.09657 (13)	0.37809 (8)	C(20)	−0.1046 (34)	0.4012 (32)	0.0644 (21)
C(1)	0.5813 (19)	0.1430 (20)	0.2425 (12)	C(21)	−0.1640 (25)	0.4286 (27)	0.2110 (17)
C(2)	0.4137 (19)	0.3361 (19)	0.2622 (11)	C(22)	−0.0726 (25)	−0.1392 (18)	0.2595 (13)
C(3)	0.1660 (20)	0.3558 (24)	0.3196 (14)	C(23)	0.0673 (34)	−0.2508 (20)	0.1877 (18)
C(4)	0.0019 (24)	0.1702 (23)	0.3663 (15)	C(24)	−0.0389 (20)	−0.1781 (22)	0.3335 (14)
C(5)	0.5135 (20)	0.1919 (22)	0.4164 (13)	N(1)	0.3213 (14)	0.2269 (13)	0.0991 (8)
C(6)	0.4934 (17)	−0.0475 (19)	0.3718 (11)	N(2)	0.3461 (14)	−0.0136 (14)	0.1497 (8)
C(7)	0.3016 (31)	0.2073 (25)	0.4640 (14)	N(3)	−0.0115 (15)	0.2385 (14)	0.1776 (9)
C(8)	0.2472 (25)	−0.0253 (22)	0.4269 (11)	N(4)	0.0478 (14)	−0.0026 (14)	0.2221 (9)
C(9)	0.3066 (19)	0.1277 (19)	0.0364 (12)	O(1)	0.6980 (15)	0.1240 (21)	0.2639 (12)
C(10)	0.3256 (19)	−0.0052 (18)	0.0662 (11)	O(2)	0.4287 (21)	0.4447 (15)	0.2882 (11)
C(11)	−0.0900 (20)	0.1410 (19)	0.1341 (13)	O(3)	0.1898 (18)	0.4597 (14)	0.3445 (12)
C(12)	−0.0618 (18)	0.0084 (21)	0.1580 (12)	O(4)	−0.0547 (31)	0.1763 (29)	0.4274 (15)
C(13)	0.3251 (23)	0.3710 (18)	0.0698 (13)	O(5)	0.6110 (18)	0.2449 (20)	0.4473 (12)
C(14)	0.4718 (30)	0.4033 (30)	0.0518 (22)	O(6)	0.5779 (17)	−0.1264 (16)	0.3732 (10)
C(15)	0.2092 (32)	0.3988 (24)	−0.0043 (20)	O(7)	0.2819 (21)	0.2631 (25)	0.5220 (10)
C(16)	0.3809 (24)	−0.1547 (17)	0.1814 (13)	O(8)	0.1966 (20)	−0.1055 (19)	0.4613 (11)

Preparation of Glyoxal Bis(neopentylimine) (2,2,9,9-Tetramethyl-4,7-diazadeca-4,6-diene). An aqueous solution of glyoxal (17.5 mL, 100 mmol) was added dropwise to a stirred solution of neopentylamine (200 mmol in 200 mL of toluene) at 60 °C. The reaction mixture was stirred for 1 h at 80 °C, and after it was cooled, the toluene was washed twice with 100 mL of water. After the solution was dried, the solvent was removed under vacuum, yielding a sticky yellow oil. The yellow oil was extracted with 150 mL of pentane, and the crude product was obtained by crystallization at −70 °C. Recrystallization from pentane produced colorless crystals of the product in 80% yield that melt at room temperature to give a viscous colorless liquid.

Preparation of $Ru(CO)_3$(DAB) [DAB = Glyoxal Bis(diisopropylmethylimine), Glyoxal Bis(mesitylimine)]. $Ru_3(CO)_{12}$ (320 mg, 0.5 mmol) and DAB were refluxed in 30 mL of heptane for 3 h. The intense red solution was filtered after cooling, and the crude product precipitated at −70 °C. Recrystallization from pentane at −70 °C gave black metallic glittering crystals in 60% yield.

Preparation of $Ru_3(CO)_8$(DAB) [DAB = Glyoxal Bis(isobutylimine), Glyoxal Bis(neopentylimine)]. $Ru_3(CO)_{12}$ (320 mg, 0.5 mmol) and DAB (0.5 mmol) were refluxed for 3 h in 30 mL of toluene. The intense red solution was filtered, and crystallization started at room temperature. Complete precipitation was achieved after 24 h at −70 °C. Recrystallization from diethylether–pentane (1:1 v/v) produced red crystals in 80% yield.

Preparation of $Ru_4(CO)_8(DAB)_2$ [DAB = Glyoxal Bis(isopropylimine), Glyoxal Bis(cyclohexylimine)]. $Ru_3(CO)_{12}$ (320 mg, 0.5 mmol) and DAB (0.75 mmol) were refluxed for 14 h (R = isopropyl) or 24 h (R = cyclohexyl) in 30 mL of heptane. The crude product precipitated when the reaction mixture was cooled down and a green powder was filtered off. This residue was washed with pentane until the filtrate remained colorless. The product was extracted with diethyl ether and was precipitated at −70 °C. Recrystallization from diethyl ether or toluene (R = cyclohexyl) gave dark green crystals in nearly quantitative yield.

Preparation of $Ru_4(CO)_8(DAB)_2$ [DAB = Glyoxal Bis(isobutylimine), Glyoxal Bis(neopentylimine)]. $Ru_3(CO)_{12}$ (320 mg, 0.5 mmol) and DAB (0.75 mmol) were refluxed for 48 h in 30 mL of pentane. The crude product precipitated after cooling of the reaction mixture and was filtered off. The product was separated by column chromatography using a silica column of 1 × 30 cm. The silica was previously dried and activated by heating it for 3 h under vacuum at 180 °C. Dichloromethane–hexane (1:1 v/v) was used as eluant, and the green fraction was collected. The solvent was removed by suction and the crude product was crystallized from diethyl ether at −70 °C to yield a small amount (less than 5%) of dark green crystals. The main product was $Ru_3(CO)_8$(DAB) as reported above.

Attempted Syntheses of $Ru_4(CO)_8$[glyoxal bis(*tert*-butylimine)]$_2$. $Ru_3(CO)_{12}$ (320 mg) and DAB (126 mg) were refluxed for 72 h in 30 mL of pentane. After cooling of the reaction mixture, small amounts of $Ru_2(CO)_5$[bis[μ-(1,2-bis(*tert*-butylimino)ethane-*N*,*N*')]] precipitated and was characterized by comparison of the spectroscopic data with the literature values,[5,7] and some insoluble material was found. The main product, however, was $Ru_2(CO)_6$(DAB).[5,7] Attempts using octane as a solvent resulted only in considerable decomposition, without any formation of the desired product.

Elemental analyses gave satisfactory results (deposited as supplementary material). All the complexes have been characterized by field-desorption mass spectrometry, and the molecular ions were in agreement with the calculated molecular weights.

Crystal Structure Determination of [Diglyoxal Bis(isopropylimine)]octacarbonyltetraruthenium. The green crystals obtained from a dilute dichloromethane solution at −70 °C were monoclinic with two molecules of $Ru_4(CO)_8$[*i*-Pr-N=CHCH=N-*i*-Pr]$_2$ in the unit cell of dimensions a = 9.506 (1) Å, b = 9.952 (3) Å, c = 16.625 (4) Å, and β = 94.975°. The space group is *Pn*.

A total of 4684 reflections were collected on a Nonius CAD 4 diffractometer, using graphite-monochromated Mo Kα radiation. A total of 3251 reflections were above the background level ($I > 2.55$).

The ruthenium atoms were located by means of a Patterson function, and from a subsequent difference Fourier synthesis, based on the phases of the ruthenium contributions, the remaining nonhydrogen atoms were obtained. The refinement was carried out by means of anisotropic block-diagonal least-squares calculations and converged to R = 0.048 for the 3251 observed reflections. The hydrogen atoms could not be located.

A weighting scheme $w = [6 + F_o + 0.0042F_o^2]^{-1}$ was used, and the anomalous dispersion of Ru was taken into account.

Absorption correction was not applied (μ = 19.04 cm^{-1}). In the final difference Fourier synthesis, no significant features appeared which justifies that absorption was neglected.

The final coordinates are listed in Table I; the temperature factors and the structure factors have been deposited as supplementary material.

Results

Molecular Structure of [Diglyoxal bis(isopropylimine)]-octacarbonyltetraruthenium. The molecular structure of the complex with the atomic numbering is shown in Figure 1, and a stereoview is given in Figure 2. Bond angles and bond lengths are given in Tables II and III, respectively.

The tetranuclear cluster contains five intermetallic separations which can be envisaged as bond distances (Å) Ru(1)–Ru(2) 2.848 (2), Ru(1)–Ru(3) 2.838 (2), Ru(2)–Ru(3) 2.994 (2), Ru(2)–Ru(4) 2.838 (2), and Ru(3)–Ru(4) 2.846 (2). However, Ru(2)–Ru(3) is slightly longer than the four other Ru–Ru bonds and is also significantly longer than the Ru–Ru bonds in $Ru_4(CO)_{13}H_2$, $Ru_4(CO)_{11}$(cyclooctene-5-yne), $Ru_4(CO)_{10}$(cyclododecatetraene), and $Ru_4(CO)_9$(4,6,8-trimethylazulene).[13] In these complexes, the Ru–Ru bond lengths vary between 2.752 and 2.939 Å. The four ruthenium atoms in $Ru_4(CO)_8(DAB)_2$ appear in a butterfly arrangement

(13) Chini, P.; Heaton, B. T. *Top. Curr. Chem.* **1977**, *74*.

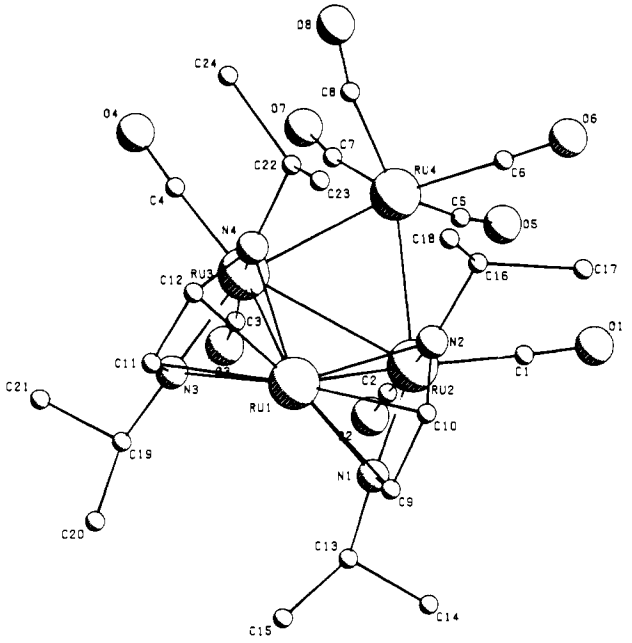

Figure 1. Molecular structure of $Ru_4(CO)_8$[glyoxal bis(isopropylimine)]$_2$ with the atomic numbering.

with a dihedral angle of 142.2° between Ru(1)–Ru(2)–Ru(3) and Ru(2)–Ru(3)–Ru(4). this is illustrated by the Newman prejection along Ru(2)–Ru(3) (Figure 3a). The angles (degrees) in the metal core are Ru(2)–Ru(1)–Ru(3) 63.59 (4), Ru(1)–Ru(2)–Ru(3) 57.98 (4), Ru(1)–Ru(2)–Ru(4) 106.98 (4), and Ru(2)–Ru(4)–Ru(3) 63.56 (4) (see also Table III).

The total number of valence electrons in the cluster is 64, and since tetranuclear clusters satisfy the 18e rule,[13] the complex should contain four delocalized metal–metal bonds. Therefore, Ru(2)–Ru(3) should not be considered as a 2e–2c bond, which is in accordance with the relative large metal–metal separation (2.994 Å). However, electron delocalization along five intermetallic axes results in a weak bonding intraction between Ru(2)–Ru(3). Ru(1)–Ru(2) and Ru(1)–Ru(3) are both bridged by a DAB ligand. The bond lengths (Å) are Ru(1)–N(1) 2.21 (1), Ru(1)–N(2) 2.24 (1), Ru(1)–C(9) 2.24 (2), Ru(1)–C(10) 2.29 (1), Ru(2)–N(1) 2.07 (1), Ru(2)–N(2) 2.20 (1), Ru(1)–N(3) 2.25 (1), Ru(1)–N(4) 2.28 (1), Ru(1)–C(11) 2.26 (2), Ru(1)–C(12) 2.24 (2), Ru(2)–N(3) 2.11 (1), and Ru(3)–N(4) 2.10. Both DAB ligands can be regarded as chelates to Ru(2) and Ru(3) and as η^2-C=N,η^2-C=N′ donors with respect to Ru(1). Consequently, the two 1,4-diazabutadiens act as 8e donors, being σ-N,σ-N′,η^2-C=N,η^2-C=N′ coordinated. This coordination mode has recently been observed in $Ru_2(CO)_4(DAB)(\mu$-HC≡CH) complexes.[2,3]

Due to the butterfly arrangement of the metal core, there is no symmetry plane perpendicular to the DAB ligand. This dissymmetry within the ligands is discussed in relation to the ^{1}H NMR data in the next section.

The two DAB ligands form five-membered rings with Ru(2) and Ru(3), and these can formally be regarded as η^5-coordinating ligands with respect to Ru(1). The structural relation with $(Cp)_2M$ molecules is illustrated by Figure 3b, showing a perspective view of the molecule along the Ru(1)–Ru(4) axis and omitting the CO and isopropyl groups.

The cluster contains eight terminal carbonyl groups: four are located on Ru(4), two on Ru(2), and two on Ru(3). Interestingly, Ru(1) does not carry carbonyl groups.

^{1}H NMR Data. The chemical shifts of the imine hydrogen atoms strongly depend upon the coordination mode of the DAB ligand. Values between approximately 7 and 9 ppm are indicative for coordination via the lone pairs on the nitrogen

Table II. Selected Bond Angles (Deg) (Esd's in Parentheses)

Metal Core			
Ru(1)-Ru(2)-Ru(3)	57.98 (4)	Ru(2)-Ru(1)-Ru(3)	63.59 (4)
Ru(1)-Ru(3)-Ru(2)	58.43 (4)	Ru(2)-Ru(4)-Ru(3)	63.56 (4)
Ru(1)-Ru(2)-Ru(4)	106.98 (6)	Ru(2)-Ru(3)-Ru(4)	58.09 (4)
Ru(1)-Ru(3)-Ru(4)	107.14 (6)	Ru(3)-Ru(2)-Ru(4)	58.35 (4)
Metal–Carbonyl Skeleton			
Ru(2)-C(1)-O(1)	175 (2)	C(3)-Ru(3)-Ru(4)	148.1 (5)
Ru(2)-C(2)-O(2)	176 (2)	C(4)-Ru(3)-Ru(1)	147.0 (6)
Ru(3)-C(3)-O(3)	174 (2)	C(4)-Ru(3)-Ru(2)	151.2 (7)
Ru(3)-C(4)-O(4)	171 (2)	C(4)-Ru(3)-Ru(4)	93.9 (7)
Ru(4)-C(5)-O(5)	173 (2)	C(5)-Ru(4)-C(6)	83.6 (8)
Ru(4)-C(6)-O(6)	174 (2)	C(5)-Ru(4)-C(7)	73.3 (11)
Ru(4)-C(7)-O(7)	170 (2)	C(5)-Ru(4)-C(8)	131.9 (9)
Ru(4)-C(8)-O(8)	170 (2)	C(6)-Ru(4)-C(7)	134.3 (9)
C(1)-Ru(2)-C(2)	88.7 (8)	C(6)-Ru(4)-C(8)	86.8 (9)
C(1)-Ru(2)-Ru(1)	146.7 (6)	C(7)-Ru(4)-C(8)	80.7 (10)
C(1)-Ru(2)-Ru(3)	143.5 (6)	C(5)-Ru(4)-Ru(2)	92.2 (7)
C(1)-Ru(2)-Ru(4)	85.2 (6)	C(5)-Ru(4)-Ru(3)	131.5 (7)
C(2)-Ru(2)-Ru(1)	123.1 (6)	C(6)-Ru(4)-Ru(2)	91.4 (5)
C(2)-Ru(2)-Ru(3)	85.3 (6)	C(6)-Ru(4)-Ru(3)	134.4 (5)
C(2)-Ru(2)-Ru(4)	82.1 (6)	C(7)-Ru(4)-Ru(2)	127.4 (7)
C(3)-Ru(3)-C(4)	87.0 (7)	C(7)-Ru(4)-Ru(3)	88.7 (8)
C(3)-Ru(3)-Ru(1)	119.8 (7)	C(8)-Ru(4)-Ru(2)	135.2 (6)
C(3)-Ru(3)-Ru(2)	83.2 (6)	C(8)-Ru(4)-Ru(3)	86.5 (7)
Metal–DAB Skeleton			
Ru(1)-N(1)-Ru(2)	83.1 (5)	N(1)-Ru(1)-C(12)	166.3 (6)
Ru(1)-N(1)-C(9)	72.1 (9)	N(1)-Ru(1)-N(4)	140.1 (5)
Ru(1)-N(1)-C(13)	130.8 (11)	N(2)-Ru(1)-Ru(3)	96.0 (3)
Ru(2)-N(1)-C(9)	121.0 (10)	N(2)-Ru(1)-N(3)	142.2 (5)
Ru(2)-N(1)-C(13)	121.6 (10)	N(2)-Ru(1)-R(11)	155.3 (6)
C(9)-N(1)-C(13)	114.9 (14)	N(2)-Ru(1)-C(12)	120.5 (6)
Ru(1)-N(2)-Ru(2)	79.6 (5)	N(2)-Ru(1)-N(4)	91.6 (5)
Ru(1)-N(2)-C(10)	73.9 (9)	Ru(2)-Ru(1)-N(3)	97.8 (4)
Ru(1)-N(2)-C(16)	132.5 (12)	Ru(2)-Ru(1)-C(11)	71.2 (5)
Ru(2)-N(2)-C(10)	117.3 (10)	Ru(2)-Ru(1)-C(12)	72.0 (5)
Ru(2)-N(2)-C(16)	125.6 (11)	Ru(2)-Ru(1)-N(4)	94.5 (4)
C(10)-N(2)-C(16)	114.1 (14)	C(9)-Ru(1)-Ru(3)	134.6 (5)
Ru(1)-C(9)-C(10)	73.8 (11)	C(9)-Ru(1)-N(3)	132.7 (6)
Ru(1)-C(9)-N(1)	70.4 (10)	C(9)-Ru(1)-C(11)	154.9 (7)
C(10)-C(9)-N(1)	112.8 (16)	C(9)-Ru(1)-C(12)	153.3 (7)
Ru(1)-C(10)-C(9)	69.7 (11)	C(9)-Ru(1)-N(4)	154.5 (6)
Ru(1)-C(10)-N(2)	70.5 (10)	C(10)-Ru(1)-Ru(3)	130.8 (5)
C(9)-C(10)-N(2)	114.0 (16)	C(10)-Ru(1)-N(3)	167.0 (5)
Ru(1)-N(3)-Ru(3)	80.4 (5)	C(10)-Ru(1)-C(11)	154.9 (7)
Ru(1)-N(3)-C(11)	71.6 (10)	C(10)-Ru(1)-C(12)	130.1 (7)
Ru(1)-N(3)-C(19)	130.0 (13)	C(10)-Ru(1)-N(4)	119.1 (6)
Ru(3)-N(3)-C(11)	116.9 (12)	N(3)-Ru(1)-Ru(3)	47.2 (4)
Ru(3)-N(3)-C(19)	124.9 (12)	N(3)-Ru(1)-N(4)	70.0 (5)
C(11)-N(3)-C(19)	116.2 (15)	N(3)-Ru(1)-C(11)	35.6 (6)
Ru(1)-N(4)-C(12)	73.3 (10)	N(3)-Ru(1)-C(12)	62.9 (6)
Ru(1)-N(4)-C(22)	131.4 (12)	N(4)-Ru(1)-Ru(3)	47.2 (4)
Ru(1)-N(4)-Ru(3)	82.9 (5)	N(4)-Ru(1)-C(11)	64.1 (6)
Ru(3)-N(4)-C(12)	116.8 (11)	N(4)-Ru(1)-C(12)	37.7 (6)
Ru(3)-N(4)-C(22)	122.3 (11)	Ru(3)-Ru(1)-C(11)	71.2 (5)
C(12)-N(4)-C(22)	117.1 (15)	Ru(3)-Ru(1)-C(12)	72.0 (5)
Ru(1)-C(11)-C(12)	71.0 (10)	C(11)-Ru(1)-C(12)	36.1 (7)
Ru(1)-C(11)-N(3)	72.8 (10)	N(1)-Ru(2)-C(1)	119.4 (8)
C(12)-C(11)-N(3)	115.5 (17)	N(1)-Ru(2)-C(2)	101.1 (7)
Ru(1)-C(12)-C(11)	72.9 (12)	N(1)-Ru(2)-N(2)	72.8 (5)
Ru(1)-C(12)-N(4)	69.0 (9)	N(1)-Ru(2)-Ru(3)	97.1 (4)
C(11)-C(12)-N(4)	113.2 (16)	N(1)-Ru(2)-Ru(4)	155.1 (4)
N(1)-Ru(1)-Ru(2)	46.3 (3)	N(2)-Ru(2)-C(1)	96.7 (7)
N(1)-Ru(1)-N(2)	69.4 (5)	N(2)-Ru(2)-C(2)	173.3 (7)
N(1)-Ru(1)-C(10)	65.6 (6)	N(2)-Ru(2)-Ru(3)	92.6 (4)
N(1)-Ru(1)-C(9)	37.5 (6)	N(2)-Ru(2)-Ru(4)	102.3 (4)
N(2)-Ru(1)-Ru(2)	49.5 (3)	N(3)-Ru(3)-C(3)	95.6 (7)
N(2)-Ru(1)-C(9)	63.3 (6)	N(3)-Ru(3)-C(4)	110.4 (8)
N(2)-Ru(1)-C(10)	35.6 (6)	N(3)-Ru(3)-N(4)	75.0 (5)
Ru(2)-Ru(1)-C(9)	73.1 (5)	N(3)-Ru(3)-Ru(2)	97.5 (4)
Ru(2)-Ru(1)-C(10)	73.1 (4)	N(3)-Ru(2)-Ru(4)	155.6 (4)
C(9)-Ru(1)-C(10)	36.5 (7)	N(4)-Ru(3)-C(3)	169.0 (8)
N(1)-Ru(1)-Ru(3)	98.5 (4)	N(4)-Ru(3)-C(4)	101.6 (8)
N(1)-Ru(1)-N(3)	103.4 (5)	N(4)-Ru(3)-Ru(2)	92.2 (4)
N(1)-Ru(1)-C(11)	132.0 (6)	N(4)-Ru(3)-Ru(4)	102.7 (4)

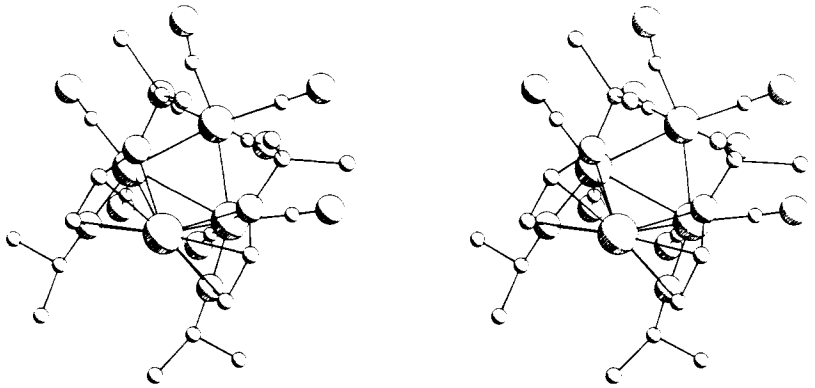

Figure 2. Stereoview of $Ru_4(CO)_8$[glyoxal bis(isopropylimine)]$_2$.

Table III. Selected Bond Lengths (Å) (Esd's in Parentheses)

Ru(1)-Ru(2)	2.848 (2)	Ru(3)-N(3)	2.11 (1)	C(5)-O(5)	1.15 (3)
Ru(1)-Ru(3)	2.838 (2)	Ru(3)-N(4)	2.10 (1)	C(6)-O(6)	1.12 (2)
Ru(2)-Ru(3)	2.994 (2)	Ru(2)-C(1)	1.85 (1)	C(7)-O(7)	1.14 (3)
Ru(2)-Ru(4)	2.838 (2)	Ru(2)-C(2)	1.78 (2)	C(8)-O(8)	1.12 (3)
Ru(3)-Ru(4)	2.846 (2)	Ru(3)-C(3)	1.96 (2)	N(1)-C(9)	1.43 (2)
Ru(1)-N(1)	2.21 (1)	Ru(3)-C(4)	1.78 (3)	N(2)-C(10)	1.39 (2)
Ru(1)-N(2)	2.24 (1)	Ru(4)-C(5)	1.82 (2)	N(3)-C(11)	1.39 (2)
Ru(1)-C(9)	2.24 (2)	Ru(4)-C(6)	1.93 (2)	N(4)-C(12)	1.43 (2)
Ru(1)-C(10)	2.29 (1)	Ru(4)-C(7)	1.92 (3)	C(9)-C(10)	1.42 (3)
Ru(1)-N(3)	2.17 (2)	Ru(4)-C(8)	1.85 (2)	C(11)-C(12)	1.40 (3)
Ru(1)-N(4)	2.18 (2)	C(1)-O(1)	1.15 (2)	N(1)-C(13)	1.52 (2)
Ru(1)-C(11)	2.26 (2)	C(2)-O(2)	1.17 (2)	N(2)-C(16)	1.53 (2)
Ru(1)-C(12)	2.24 (2)	C(3)-C(3)	1.13 (3)	N(3)-C(19)	1.52 (2)
Ru(2)-N(1)	2.07 (1)	C(4)-O(4)	1.19 (4)	N(4)-C(22)	1.50 (2)
Ru(2)-N(2)	2.20 (1)				

Table IV. ^{1}H NMR Chemical Shifts of $Ru(CO)_3$(DAB), $Ru_3(CO)_8$(DAB), $Ru_4(CO)_8(DAB)_2$, and $Ru_2(CO)_4$(μ-acetylene)(DAB) (ppm relative to Me_4Si)

complex	δ(substituent)	δ(H_{imine})
$Ru(CO)_3$[glyoxal bis(diisopropylmethylimine)][a]	3.83 (t), 2.10 (m), 0.88 (d)[c]/0.94 (d)	6.95
$Ru(CO)_3$[glyoxal bis(mesitylimine)][b]	2.20 (*o*-CH_3), 2.35 (*p*-CH_3), 6.93 (aromatic)	7.10
$Ru_3(CO)_8$[glyoxal bis(isobutylimine)][b]	3.07 (d), 1.90 (m), 0.90 (d)/1.04 (d)	5.86
$Ru_3(CO)_8$[glyoxal bis(neopentylimine)][b]	3.01, 1.99 (J_{AX} = 13Hz),[d] 1.03	5.89
$Ru_4(CO)_8$[glyoxal bis(isopropylimine)]$_2$[b]	4.10 (sept), 1.51 (d)/1.26 (d)	6.56
$Ru_4(CO)_8$[glyoxal bis(cyclohexylimine)]$_2$[b]	3.8 (m), 1-2 (br m)	6.49
$Ru_4(CO)_8$[glyoxal bis(isobutylimine)]$_2$[b]	0.94 (d), 1.14 (d), 2.28 (m), 3.57 (m)	6.21
$Ru_4(CO)_8$[glyoxal bis(neopentylimine)]$_2$[b]	1.01, 1.14,[e] 3.48, 2.29 (J_{AB} = 12Hz),[d] 3.70, 2.47 (J_{AB} = 12Hz)[d]	5.99, 6.20
$Ru_2(CO)_4$(HC≡CH)[glyoxal bis(isopropylimine)][b]	0.63/1.19 (d), 2.23 (m), 7.50, 8.22 (HC≡CH)	6.17
$Ru_2(CO)_4$(HC≡CH)[glyoxal bis(cyclohexylimine)][b]	1-2 (br m), 7.49, 8.28 (HC≡CH)	6.22

[a] Solvent is toluene-d_8. [b] Solvent is $CDCl_3$. [c] Values separated by a vertical bar correspond with diastereotopic pairs. [d] The methylene signal appears as an AB pattern due to anisochronous hydrogen atoms. [e] Multiplet partially obscured by the signal at 1.10 ppm.

atoms.[14,15] For $Ru(CO)_3$[glyoxal bis(diisopropylmethylimine)] and $Ru(CO)_8$[glyoxal bis(mesitylimine)], the imine hydrogen resonances are found at 6.95 (in toluene-D_8) and 7.10 ppm, respectively, indicating that the DAB ligand in these mononuclear complexes acts as a bidentate. Analogous results have been obtained for $Fe(CO)_3$(DAB) complexes which justify the conclusion that the mononuclear ruthenium complexes are isostructural with the iron derivatives. The structure is given in Figure 4.

The ^{1}H NMR signals for the imine hydrogen atoms in $Ru_4(CO)_8(DAB)_2$ complexes are found near 6.5 ppm. This is about 1.5-2.0 ppm shifted to higher field as compared with the values obtained for the free ligands and confirms the interpreparation of the crystal structure concerning the η^2-C=N,η^2-C=N′ coordination of both DAB ligands.

Similar chemical shifts have been obtained for $Ru_2(CO)_4$-(μ-HC≡CH)(DAB) complexes in which the DAB also acts as an 8e donor. The ^{1}H NMR data of these latter complexes are included in Table IV, listing the NMR results for Ru-

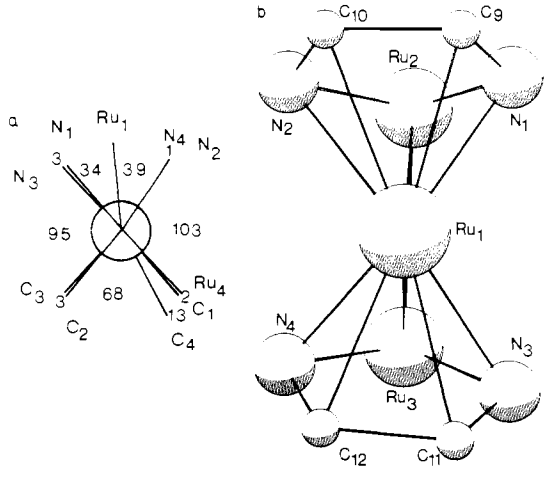

Figure 3. (a) Newman projection along Ru(2)-Ru(3). (b) Perspective view of the [Ru(1)-Ru(2)-Ru(3)(DAB)$_2$] fragment of the molecule, showing the relation with η^5-donor ligands.

(14) Staal, L. H.; van Koten, G.; Vrieze, K. *J. Organomet. Chem.* **1979**, *175*, 73-86.
(15) tom Dieck, H.; Renk, I. W.; Franz, K. D. *J. Organomet. Chem.* **1975**, *94*, 417-424.
(16) Staal, L. H.; Polm, L. H.; Vrieze, K. *Inorg. Chim. Acta* **1980**, *40*, 165-170.

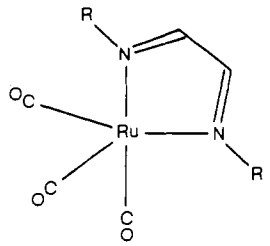

Figure 4. Structure of $Ru(CO)_3(DAB)$.

$(CO)_3(DAB)$, $Ru_3(CO)_8(DAB)$, and $Ru_4(CO)_8(DAB)_2$ complexes.

The crystal structure of $Ru_4(CO)_8$[glyoxal bis(isopropylimine)]$_2$ showed that in the solid state the two halves of each ligand are inequivalent. With the assumptions that the solid-state structure and that the structure of the dissolved molecules are the same, the two imine hydrogen atoms and the two alkyl substituents should be inequivalent. In the ^1H NMR spectrum of $Ru_4(CO)_8$[glyoxal bis(neopentylimine)]$_2$, indeed, two separate sets of resonances can be observed for the two inequivalent ligand halves. Accordingly, this complex is rigid on the NMR time scale at room temperature.

However, at room temperature, the ^1H NMR spectra of $Ru_4(CO)_8$[glyoxal bis(isopropylimine)]$_2$ and $Ru_4(CO)_8$[glyoxal bis(cyclohexylimine)]$_2$ show only one set of sharp signals for the nonequivalent ligand halves, indicating a dynamic process within these clusters. Therefore the ^1H NMR spectra of $Ru_4(CO)_8$[glyoxal bis(cyclohexylimine)]$_2$ have been recorded at low temperatures in dichloromethane-d_2. Indeed, the sharp singlet at 6.70 ppm for the imine hydrogen atoms (6.49 ppm in $CDCl_3$ solution) broadens at −40 °C, and at −60 °C two broad resonances appear at 6.98 and 6.48 ppm, respectively. At −102 °C, the two separate signals for the two nonequivalent imine hydrogen sites are still slightly broadened. Simultaneously, the resonances of the cyclohexyl group split into two separate sets. This can best be observed by the splitting of the signal for the α-hydrogen atoms of the cyclohexyl rings.

Interestingly, for $Ru_4(CO)_8$[glyoxal bis(isobutylimine)]$_2$, two separate sets of signals are observed at room temperature for the isobutyl groups, while the imine hydrogen atoms still give one signal at 6.2 ppm, although slightly broadened.

The ^1H NMR results for the $Ru_4(CO)_8(DAB)_2$ complexes demonstrate the dissymmetry in the DAB ligands and that at room temperature a two-sites exchange process reaches the limit of the fast exchange for the isopropyl and cyclohexyl derivatives. Furthermore, the activation energy for the exchange process increases with increasing bulkiness of the alkyl substituents attached to the imine nitrogen atoms: cyclohexyl < isobutyl < neopentyl.

According to the Newman projection (Figure 3) of $Ru_4(CO)_8$[glyoxal bis(isopropylimine)]$_2$, both DAB ligands are almost symmetrical with respect to the Ru(1)–Ru(2) and Ru(1)–Ru(3) bonds. The asymmetry within the ligands is caused by the butterfly arrangement of the metal skeleton. Therefore the fluxional behavior of the molecule is determined by a motion from the $Ru(CO)_4$ fragment from above to underneath the Ru(1)–Ru(2)–Ru(3) plane, thereby creating a kind of flying movement of the butterfly skeleton. In the transition state, the metal core should be planar (see Figure 5).

The ^1H NMR chemical shifts for the imine hydrogen atoms of $Ru_3(CO)_8$[glyoxal bis(isobutylimine)] and $Ru_3(CO)_8$[glyoxal bis(neopentylimine)] are 5.86 and 5.89 ppm, respectively. These values are in the region of the chemical shifts of the imine hydrogen atoms of σ-N,σ-N′,η^2-C=N,η^2-C=N′-coordinated DAB ligands in $Ru_4(CO)_8(DAB)_2$ and $Ru_2(CO)_4$(DAB)(HC≡CH) complexes[2,3] (see Table IV). This indicates that the $Ru_3(CO)_8(DAB)$ complexes contain 8e-donating

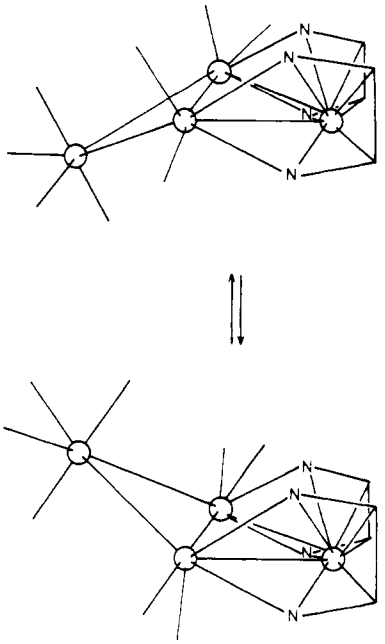

Figure 5. Schematic presentation of the proposed exchange mechanism in $Ru_4(CO)_8(DAB)_2$ clusters.

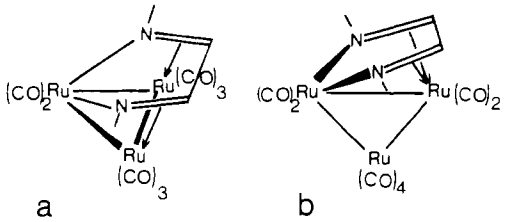

Figure 6. Two possible structures for $Ru_3(CO)_8(DAB)$.

σ-N,σ-N′,μ^2-C=N,η^2-C=N′-coordinated 1,4-diazabutadienes, and in fact the effective atomic number rule requires that the DAB ligands in these trinuclear clusters are 8e donors. In principle two isomeric structures of $Ru_3(CO)_8(DAB)$ can be proposed on the basis of the ^1H NMR data. The DAB ligand in the proposed structure as depicted in Figure 6a is bonded to each of the three metal centers of the cluster, whereas the ligand in the structure shown in Figure 6b is bonded to two metals. This latter structure would be in analogy with two precedents of 8e-donor modes of 1,4-diazabutadienes in $Ru_4(CO)_8(DAB)_2$ (this work) and $Ru_2(CO)_4(DAB)(\mu$-HC≡CH).[14] However, on the basis of present results, one cannot discriminate between structure 6a and 6b (a crystal structure determination is in progress).

The ^1H NMR patterns of prochiral substituents attached to the imine nitrogen atoms of the coordinated DAB ligands reflect the absence of a symmetry plane through the N=C-C=N skeleton. This is illustrated for the $Ru_4(CO)_8(DAB)_2$ clusters by the ^1H NMR pattern of the four isopropyl groups in $Ru_4(CO)_8$[glyoxal bis(isopropylimine)]$_2$ (see Figure 7a) and for the $Ru_3(CO)_8(DAB)$ clusters by the ^1H NMR pattern of the CH_2 fragment of the neopentyl groups in $Ru_3(CO)_8$[glyoxal bis(neopentylimine)] (see Figure 7b).

The CO Stretching Frequencies. The ν(CO) frequencies of the complexes are listed in Table V. For $Ru(CO)_3$[glyoxal bis(diisopropylimine)], one sharp band is found at 2040 cm^{-1} (A_1) and one broad, very intense band at 1969 cm^{-1} (E), showing that the $Ru(CO)_3$ unit possesses pseudo-C_{3v} symmetry. For $Ru(CO)_3$[glyoxal bis(mesitylimine)], three bands have been observed at 2051, 1988, and 1976 cm^{-1}. The band below 2000 cm^{-1} has split ($A_1 + B_1$), indicating that the $Ru(CO)_3$ unit in this complex has a C_{2v} symmetry. An analogous disparity between aromatic and aliphatic DAB ligands has been

Table V. ν(CO) Stretching Frequencies (cm^{-1}) of $Ru(CO)_3(DAB)$, $Ru_3(CO)_8(DAB)$, and $Ru_4(CO)_8(DAB)_2$

$Ru(CO)_3$[glyoxal bis(diisopropylmethylimine)][a]	2040 (s),[d] 1969 (s)
$Ru(CO)_3$[glyoxal bis(xylylimine)][c]	2053 (s), 1991 (s), 1978 (s)
$Ru(CO)_3$[glyoxal bis(mesitylimine)][a]	2051 (s), 1988 (s), 1976 (s)
$Ru_4(CO)_8$[glyoxal bis(isopropylimine)]$_2$[b]	2016 (w), 1995 (vs), 1946 (s), 1929 (s), 1899 (m)
$Ru_4(CO)_8$[glyoxal bis(cyclohexylimine)]$_2$[b]	2014 (w), 1993 (s), 1963 (s), 1928 (s), 1898 (m)
$Ru_4(CO)_8$[glyoxal bis(isobutylimine)]$_2$[b]	2021 (vw), 1998 (s), 1966 (s), 1935 (s), 1901 (m)
$Ru_4(CO)_8$[glyoxal bis(neopentylimine)]$_2$[b]	2032 (w), 2004 (vs), 1971 (s), 1941 (m), 1914 (m)
$Ru_3(CO)_8$[glyoxal bis(isobutylimine)][a]	2078 (w), 2044 (s), 1998 (s),[e] 1988 (m), 1979 (m), 1943 (w), 1926 (vw)
$Ru_3(CO)_8$[glyoxal bis(neopentylimine)][a]	2082 (m), 2058 (s), 2028 (s), 2007 (s), 1998 (sh), 1977 (m), 1949 (w), 1952 (m)

[a] Solvent is pentane. [b] Solvent is dichloromethane. [c] Unstable sample recorded as heptane solution. [d] Key: vs = very strong, s = strong, m = medium, w = weak, vw = very weak. [e] Shoulder on higher wavenumber.

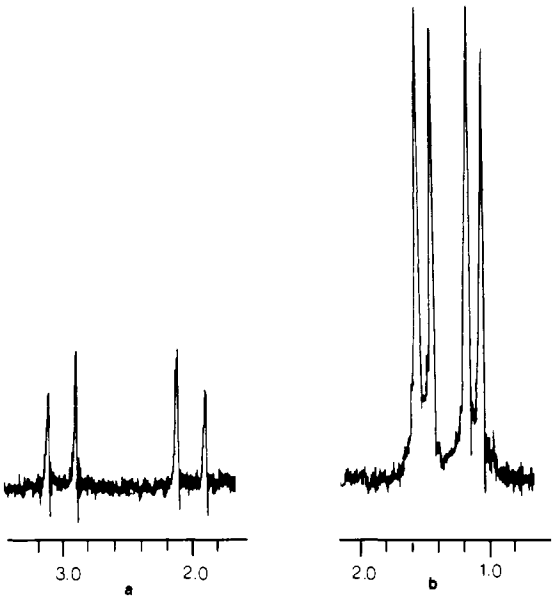

Figure 7. (a) ^1H NMR pattern of the isopropyl groups in $Ru_4(CO)_8$[glyoxal bis(isopropylimine)]$_2$. (b) ^1H NMR pattern of the CH_2 fragments of the neopentyl groups in $Ru_3(CO)_8$[glyoxal bis(neopentylimine)].

observed in $Fe(CO)_3(DAB)$ complexes.[17,18]

For the trinuclear clusters $Ru_3(CO)_8(DAB)$, eight bands can be observed in the carbonyl stretching region. Due to low symmetry in the complexes (C_s), an assignment is not possible without ^{13}CO labeling. The same applies to the tetranuclear clusters for which are found four broad intense bands between 2000 and 1890 cm^{-1} and a weak sharp band at 2020 cm^{-1} (approximate values; see also Table V).

Discussion

(i) Complex Formation. The formation of the complexes strongly depends upon the substituents attached to the imine nitrogen atoms of the ligands. In Table VI a series of glyoxal bis(imine) derivatives is listed together with the ruthenium carbonyl complexes which have been isolated for these ligands.

Mononuclear complexes $Ru(CO)_3(DAB)$ have been isolated for glyoxal bis(diisopropylmethylimine) (a) and glyoxal bis(mesitylimine) (c) and could furthermore be detected in solution for glyoxal bis(xylylimine) (b). These ligands have in common that the ortho positions (or the 2,4-positions for the alkyl group) are occupied by methyl groups.

Binuclear ruthenium carbonyl complexes containing one DAB ligand, $Ru_2(CO)_6(DAB)$, have been obtained for glyoxal bis(isopropylimine) (d), glyoxal bis(cyclohexylimine) (e), and glyoxal bis(*tert*-butylimine). In these complexes the DAB ligands behave like 6e donors, being σ-N,μ^2-N′,η^2-C=N′ coordinated[5,7] (see Figure 8a). Binuclear ruthenium carbonyl

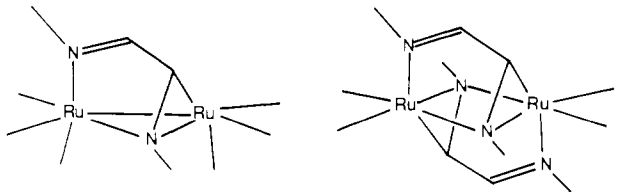

Figure 8. Structures of $Ru_2(CO)_6(DAB)$ (left) and $Ru_2(CO)_4(DAB)_2$ (right).

complexes with two DAB ligands in the 6e-donor mode have been prepared for glyoxal bis(isopropylimine) (d), glyoxal bis(cyclohexylimine) (e), and glyoxal bis(*p*-tolylimine) (i) (see Figure 8b).[5] All attempts to prepare a $Ru_2(CO)_4(DAB)_2$ complex with glyoxal bis(*tert*-butylimine) failed.

The rate constant for the formation of $Ru_2(CO)_6(DAB)$ complexes has been determined by means of reaction monitoring with high-performance liquid chromatography, and it was shown that glyoxal bis(*tert*-butylimine) was at least a factor of 40 less reactive than glyoxal bis(isopropylimine).[19]

Trinuclear ruthenium carbonyl DAB complexes have been obtained for glyoxal bis(isobutylimine) (f) and glyoxal bis(neopentylimine) (g). These complexes can be regarded as direct substitution products of the *triangulo*-ruthenium dodecacarbonyl complex. Glyoxal bis(isobutylimine) and glyoxal bis(neopentylimine) have in common that, although the substituents are bulky aliphatic groups, the bulkiness is not restricted to one side of the N=CC=N plane.

Tetranuclear ruthenium carbonyl DAB complexes have been obtained in a good yield for glyoxal bis(isopropylimine) (d) and glyoxal bis(cyclohexylimine) (e) and as trace products for glyoxal bis(isobutylimine) (f) and glyoxal bis(neopentylimine) (g). The formation of $Ru_4(CO)_8$[glyoxal bis(isopropylimine)]$_2$ and $Ru_4(CO)_8$[glyoxal bis(cyclohexylimine)]$_2$ was monitored by means of IR spectroscopy in the carbonyl stretching region, and the characteristic ν(CO) pattern of the $Ru_2(CO)_6(DAB)$ complexes[5,6,7] appeared shortly after the reaction was started. This provides evidence that the $Ru_2(CO)_6(DAB)$ complexes are intermediates in the formation of the $Ru_4(CO)_8(DAB)_2$ clusters, according to eq 1. (The reaction with 3 equiv of DAB

$$\begin{aligned} Ru_3(CO)_{12} + {}^3/_2\,DAB \xrightarrow{\Delta T} {}& {}^3/_2\,Ru_2(CO)_6(DAB) + 3CO \\ & \downarrow \Delta T \\ & {}^3/_4\,Ru_4(CO)_8(DAB)_2 + 3CO \end{aligned} \qquad (1)$$

leads to the formation of $Ru_2(CO)_5(IAE)$ complexes (see also ref 5).)

The formation of the cluster by dimerization of $Ru_2(CO)_6(DAB)$ requires the dissociation of at least one η^2 bond between a DAB ligand and a ruthenium atom in order to create η^4 coordination between one ruthenium atom and two DAB ligands. Furthermore, migration of a CO group is required in order to form a $Ru(CO)_4$ unit. The fact that in the

(17) Orlopp, A.; tom Dieck, H. *Angew. Chem.* **1975**, *87*, 246–247.
(18) Liebfritz, D.; tom Dieck, H. *J. Organomet. Chem.* **1976**, *105*, 255–261.
(19) Gast, C. H.; Kraak, J.; Staal, L. H.; Vrieze, K. *J. Organomet. Chem.* **1981**, *208*, 225–238.

Table VI

ligand	complexes	ligand	complexes
a 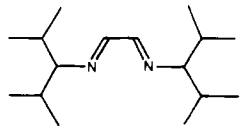	$Ru(CO)_3(DAB)$	f 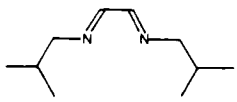	$Ru_3(CO)_8(DAB)$ $Ru_4(CO)_8(DAB)_2$
b 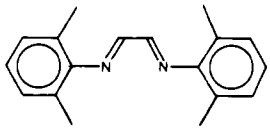	$Ru(CO)_3(DAB)$	g 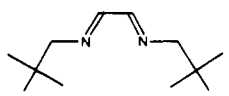	$Ru_3(CO)_8(DAB)$ $Ru_4(CO)_8(DAB)_2$
c 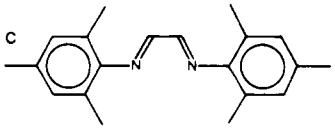	$Ru(CO)_3(DAB)$	h 	$Ru_2(CO)_6(DAB)$
d 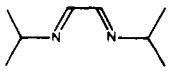	$Ru_2(CO)_6(DAB)$ $Ru_2(CO)_4(DAB)_2$ $Ru_4(CO)_8(DAB)_2$	i 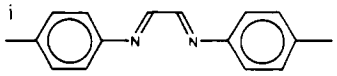	$Ru_2(CO)_4(DAB)_2$
e 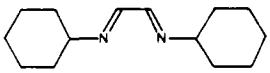	$Ru_2(CO)_6(DAB)$ $Ru_2(CO)_4(DAB)_2$ $Ru_4(CO)_8(DAB)_2$		

case of glyoxal bis(isopropylimine) and glyoxal bis(cyclohexylimine) the cluster is produced in nearly quantitative yield shows that the dimerization occurs via a very efficient mechanism. The nature of this mechanism, which probably involves more than one step, is still unknown.

The synthesis of the *tert*-butyl derivative of $Ru_4(CO)_8(DAB)_2$ failed. Prolonged heating of $Ru_3(CO)_{12}$ and glyoxal bis(*tert*-butylimine) produced only $Ru_2(CO)_6$[glyoxal bis(*tert*-butylimine)].

(ii) Substituent Effects. For a better understanding of the influences of the 1,4-substituents attached to DAB, on the complex formation, these influences have to be divided into steric factors and electronic factors. It will be shown that the steric factors can be subdivided into internal and external repulsions.

It is important to note that σ-N,σ-N′ coordination is a prerequisite prior to η^2-C=N coordination in order to obviate the electronic repulsion between the lone pairs on nitrogen, when the ligand is in the trans–syn–trans conformation.[2] This has been demonstrated by kinetic studies on the reaction of $Ru_3(CO)_{12}$ and 1,4-diazabutadienes which indicated the formation of an unstable intermediate $[Ru_3(CO)_{10}(DAB)]$ as the first step in the reaction mechanism.[19] The 1,4-diazabutadienes in these intermediates act as σ-N,σ-N′ bidentate ligands.

The formation of mono- and binuclear complexes requires cluster breakdown, while the formation of $Ru_3(CO)_8(DAB)$ can be envisaged as a subsequent intramolecular reaction of $[Ru_3(CO)_{10}(DAB)]$, leading to stabilization of the trinuclear cluster. The isolation of $Os_3(CO)_9(DAB)$, in which we succeeded recently, supports this assumption.[6]

In glyoxal bis[diisopropylmethylimine] (a), glyoxal bis(xylylimine) (b), and glyoxal bis(mesitylimine) (c), the ortho positions (in the alkyl group the 2,4-positions) are occupied by methyl groups. Due to steric crowding, these 1,4-substituents will be in a perpendicular orientation with respect to the chelate plane, thereby screening the N=CC=N skeleton and protecting the π electrons against a subsequent attack by the metal entity. Consequently, neither a trinuclear nor a binuclear structure could be stabilized by η^2-C=N coordination and the cluster will fall apart into mononuclear fragments. The formation and stability of the mononuclear complexes is the result of external repulsion.

The difference in complex formation for the other ligands listed in Table VI can best be explained for the alkyl derivatives (d–h). It has been discussed above that DAB ligands form chelate rings with one of the ruthenium atoms in the $[Ru_3(CO)_{10}DAB]$ intermediate. These chelate rings are planar since the nitrogen atoms (and the imine carbon atoms) are sp^2 hybridized, and consequently the valence angles around nitrogen are near the idealized valence angles of 120°. However, η^2 coordination would cause sp^3 character on the imine nitrogen atoms, corresponding to a decrease of the valence angles. When there are bulky groups attached to the nitrogen atoms, a decrease of the valence angles around nitrogen would increase the steric repulsion between the imine H and the branched R group. Accordingly, the π-coordinating ability decreases with increasing bulkiness of the 1,4-substituents. This will influence not only the stability of the complexes but also the reactivity of the ligands. The expected tendency toward η^2 coordination will depend upon the branching at the α-position of the alkyl substituents: thus RCH_2 better than R_2CH better than R_3C. For the alkyl groups (d–h) listed in Table VI, the order would be isobutyl, neopentyl > isopropyl, cyclohexyl > *tert*-butyl. Interestingly, the chemical shifts of the imine hydrogen atoms in $Ru_4(CO)_8(DAB)_2$ indicate the same order when they are correlated with the extent of back-donation.

Opposite trends have been observed for the radical production by thermolysis of hydrocarbons or azoalkanes. For these reactions, the hybridization on the central carbon atoms changes from sp^3 to sp^2, and consequently an increasing bulkiness leads to a decrease of the activation energy.[20]

On the basis of these considerations, the formation of $Ru_3(CO)_8(DAB)$ and $Ru_2(CO)_6(DAB)$ can be made plausible. The isolation of small amounts of $Ru_4(CO)_8$[glyoxal bis(isobutylimine)]$_2$ and $Ru_4(CO)_8$[glyoxal bis(neopentylimine)]$_2$

(20) Rüchardt, C. *Top. Curr. Chem.* **1980**, *88*.

Figure 9. Resonance structures of the 8e-donor mode of DAB ligands.

(which are formed via dimerization of $Ru_2(CO)_6$(DAB) complexes), in addition to the corresponding $Ru_3(CO)_8$(DAB) complexes, demonstrates that $Ru_3(CO)_8$(DAB) and $Ru_2(CO)_6$(DAB) formation are competing reactions. Which of them will eventually occur in the system is determined by the activation barrier for each of the processes. Consequently, good π-bonding abilities of the DAB ligands (i.e., isobutyl and neopentyl) causes preferentially the formation of $Ru_3(CO)_8$(DAB) complexes while a decrease in the π-bonding capacity (isopropyl, cyclohexyl > *tert*-butyl) is in favor of cluster breakdown, resulting in $Ru_2(CO)_6$(DAB) formation.

It is obvious now that α branching determines the reactivity of the DAB ligands, but glyoxal bis(*p*-tolylimine) does not fit into this model. The steric influence can be compared with a cyclohexyl group, but the orientation of the aromatic ring, i.e., coplanar with the N=CC=N skeleton or twisted out of plane, will have electronic influences.

Electronic influences can also be anticipated for the aliphatic substituents but seem of less importance. Electron-donating groups attached to the imine nitrogen atoms are capable of neutralizing the polarization within the C=N bond, resulting in better π-bonding properties.[8] When this effect would dominate, glyoxal bis(*tert*-butylimine) would be a better π-bonding ligand than glyoxal bis(isopropylimine), which is in disagreement with the observed behavior.

(iii) Valence Structure. In general, σ-coordinated 1,4-diazabutadienes can be regarded either as neutral or as double-charged ligands. The valence structures depend upon the nature of the heteroatoms and upon the central metals in the chelate rings. The σ-N,σ-N′-coordinated DAB ligands remain formally 1,3-diene systems, this in disparity with, e.g., tetraazabutadienes. The coordinated tetraazabutadienes may act as neutral ligands as in $Ni((aryl)_2\text{-}N_4)_2$[21] or as double-charged ligands as in $(\eta^5\text{-}C_5H_5)Ni((p\text{-}tol)_2\text{-}N_4)$.[21] The two different formal valence structures of tetraazadienes have physical significance and can be distinguished by means of X-ray crystallography.

The crystal structures of $Ru_2(CO)_4[\mu\text{-}H{\equiv}CH]$[glyoxal bis(isopropylimine)] and $Ru_4(CO)_8$[glyoxal bis(isopropylimine)]$_2$ have established the 8e-donor mode of DAB ligands. Since 1,4-diazabutadienes are neutral ligands, the 8e-donor mode can be regarded as σ-N,σ-N′,η^2-C=N,η^2-C=N′ coordination as is schematically depicted in Figure 9a. However, analogous to the coordination of tetraazadienes, a resonance structure can be formulated involving reduction of the ligand. This is shown schematically in Figure 9b. In this structure the DAB ligand is reduced to a double-charged molecule, forming an endiamine, with an η^2-coordinated C=C bond. Although this resonance structure may have a stabilizing influence on the $\sigma,\sigma,\eta^2,\eta^2$-coordination mode of DAB ligands, it is physically indistinguishable. Due to the π donation, the C=N bond lengths will increase. This effect will become even more pronounced due to the back-donation into the LUMO of the N=CC=N skeleton which is antibonding with respect to the C=N bonds. However, the LUMO is bonding with respect to the central C—C bond, and back-donation will therefore result in a decrease of this C—C bond. The averaged C=N bond lengths in $Ru_4(CO)_8$[glyoxal bis(isopropylimine)]$_2$ are 1.41 Å, and the averaged central C—C bonds of the diimines in this compound are 1.41 Å; both illustrate this effect (see Table II).

It can be anticipated that electron-withdrawing or electron-donating properties of the 1,4-substituents may influence the valence isomerism and thereby the stability of the π bonds between the DAB ligands and the metals.

In this work, the 1,4-diazabutadienes have been derived from glyoxal, and consequently the imine carbon atoms do not carry substituents. However, 2,3-substituents on the N=CC=N skeleton may also influence the coordination behavior of DAB ligands. This has been shown before for 1,4-diazabutadienes with a methyl group attached to only one of the imine carbon atoms. π Coordination only occurred on the nonsubstituted part of the ligand.[5,8] DAB ligands with methyl groups on each imine carbon atom (diacetyl derivatives) appeared to posses very poor π-bonding capacity.[8] Therefore, in the future, more attention has to be paid to the influence of electron-withdrawing and electron-donating groups on the 2,3-positions of the N=CC=N skeleton with respect to the coordination behavior of the ligands. Furthermore, analogous steric factors as discussed for the 1,4-substituents may be expected for the 2,3-substituents.

Conclusions

It has been shown that α branching of the substituents is one of the main steric factors which determine the reactivity of the DAB ligands. The influence of electronic factors is less pronounced. An indication for small electronic differences has been found by electrochemical investigations[22] and semiempirical calculations.[23]

The eight-electron-donor mode of DAB ligands, i.e., σ-N,σ-N′,η^2-C=N,η^2-C=N′ coordination has been observed in three types of complexes, illustrating that this coordination mode does not only occur as an occasional exception but that it will probably appear more generally in bi- and polynuclear DAB complexes.

Acknowledgment. We thank Mr. Heijdenrijk for collecting the crystal data and Mr. R. H. Fokkens for recording the mass spectra. Dr G. van Koten is acknowledged for stimulating discussions.

Registry No. $Ru(CO)_3$[glyoxal bis(diisopropylmethylimine)], 78199-25-4; $Ru(CO)_3$[glyoxal bis(mesitylimine)], 78199-26-5; $Ru_3(CO)_8$[glyoxal bis(isobutylimine)], 78199-27-6; $Ru_3(CO)_8$[glyoxal bis(neopentylimine)], 78199-28-7; $Ru_4(CO)_8$[glyoxal bis(isopropylimine)]$_2$, 78199-36-7; $Ru_4(CO)_8$[glyoxal bis(cyclohexylimine)]$_2$, 78199-37-8; $Ru_4(CO)_8$[glyoxal bis(isobutylimine)]$_2$, 78199-38-9; $Ru_4(CO)_8$[glyoxal bis(neopentylimine)]$_2$, 78199-39-0; $Ru(CO)_3$[glyoxal bis(xylylimine)], 78199-29-8; glyoxal bis(diisopropylmethylimine), 59725-31-4; glyoxal bis(isobutylimine), 24764-89-4; glyoxal bis(neopentylimine), 78198-90-0; glyoxal, 107-22-2; 3-amino-2,4-dimethylpentane, 4083-57-2; isobutylamine, 78-81-9; neopentylamine, 5813-64-9; $Ru_3(CO)_{12}$, 15243-33-1.

Supplementary Material Available: Listings of elemental analyses, thermal parameters, and structure factors (23 pages). Ordering information is given on any current masthead page.

(21) Overbosch, P.; van Koten, G.; Overbeek, O. *J. Am. Chem. Soc.* **1980**, *102*, 2091–2093.
(22) tom Dieck, H.; Renk, I. W. *Chem. Ber.* **1971**, *104*, 110–130.
(23) Reinhold, J.; Benedix, R.; Birner, P.; Hennig, H. *Inorg. Chim. Acta* **1979**, *33*, 209–213.